Search for anisotropies in the arrival directions of cosmic rays above 32 EeV from Phase One of the Pierre Auger Observatory

https://arxiv.org/abs/2206.13492

UNIVERSITÀ DEGLI STUDI DI MILANO

PIERRE AUGER OBSERVATORY

Claudio Galelli for the Pierre Auger Collaboration
27th European Cosmic Ray Symposium, Nijmegen

The Pierre Auger Observatory

The largest UHECR observatory ever built - 3000 km (~Luxembourg)

1600 water Cherenkov detectors to sample the shower plane at earth (SD)

Hybrid design

24 fluorescence telescopes in 4 sites (FD)

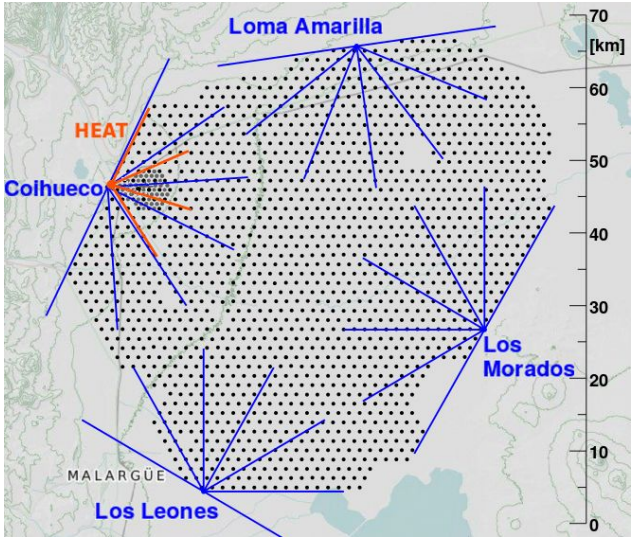

Low energy enhancements both in SD (infill) and in FD (HEAT)

85% of sky coverage, angular resolution <1° above the ankle

Exposure at the highest energies/loosest cuts: **120000 km2 yr sr** 2004-2020
40-70x larger than previous experiments (AGASA, HiRES)
9x larger than the northern complementary TA

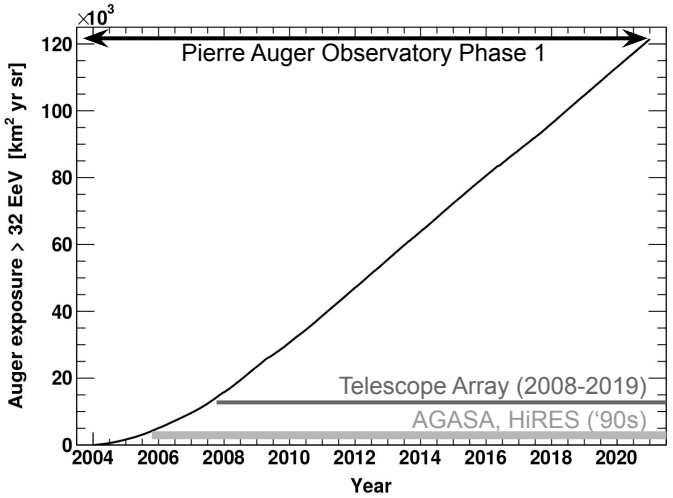

Spectrum, composition and arrival direction

Spectrum and composition observables integrate over the sphere information about
acceleration, **propagation**, **source escape spectrum**, **distance**

Spectral features (change of index) confronted with combined
spectrum-composition models are markers of source characteristics

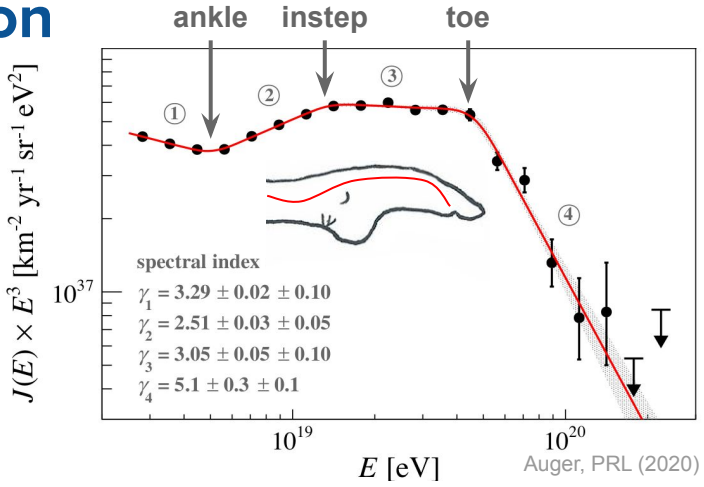

Auger, PRL (2020)

Ankle, 5 EeV
Transition from galactic
to extragalactic sources

Instep, 10-15 EeV
Peters cycle
(mass of primary CR)

Toe, 40-50 EeV
UHECR horizon (GZK)
or source exhaustion

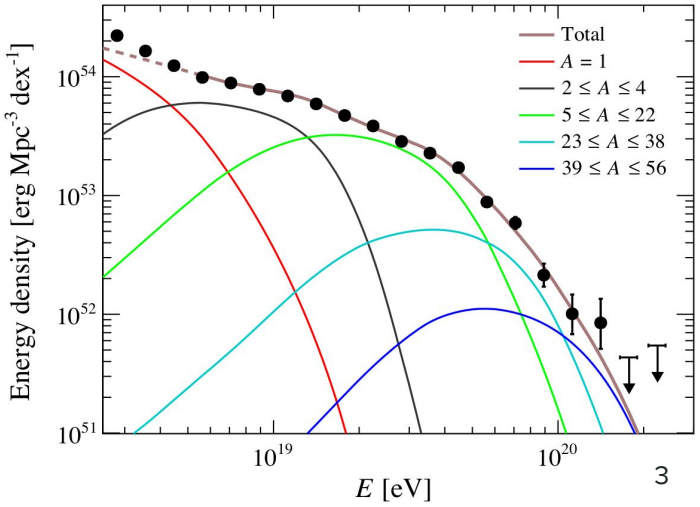

Anisotropy analyses

Break down the flux based on arrival directions
Try to **pinpoint the sources** directly

A brief history of anisotropy studies

Auger, Science 2007

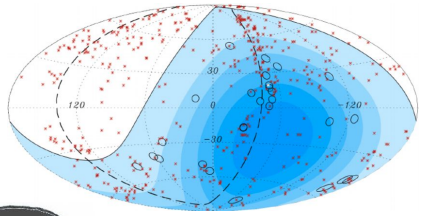

~ 27 evts ≥ 57 EeV

Auger, Science 2017

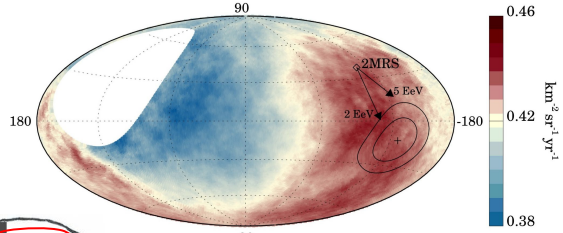

~ 32,000 evts ≥ 8 EeV

Auger, ApJL 2018

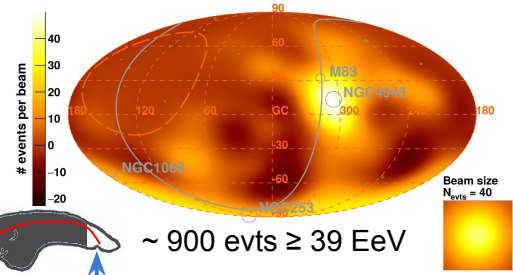

~ 900 evts ≥ 39 EeV

2007

27 events > 57 EeV

20/27 within 3°
of nearby galaxies

10 clustered
in the **Centaurus region**

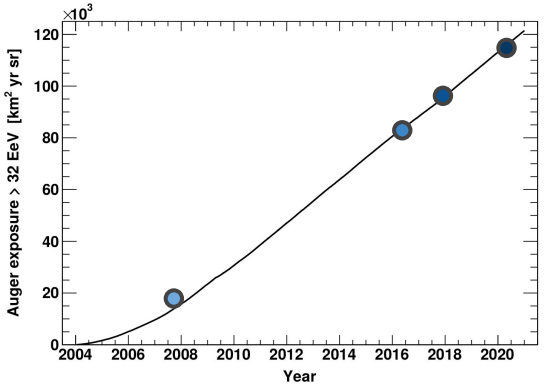

2017

32,000 evts ≥ 8 EeV

>5σ dipolar-like flux

In line with nearby
galaxy stellar mass distribution (2MRS)

2018

900 evts ≥ 39 EeV

4σ evidence for correlation
with nearby **starforming galaxies**

3σ level for other types
of galaxies

2020

2600 evts ≥ 32 EeV

Building the dataset

https://doi.org/10.5281/zenodo.6504276

Largest dataset ever built at the extreme energies: 2635 events with energy above 32 EeV

"Vertical"
2040 with zenith angle θ<60°

"Inclined"
595 with zenith angle θ>60°

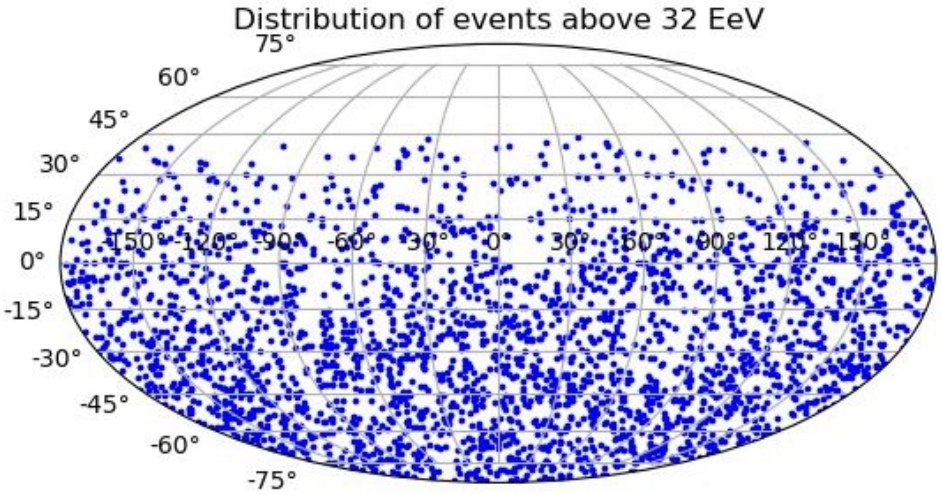

Highest energy range for dipolar searches (where dipole significance drops)

2635 above 32 EeV
647 above 50 EeV
261 above 64 EeV
36 above 100 EeV (0.1 ZeV!)
Highest energy event: 165 EeV

Building the dataset

Largest dataset ever built at the extreme energies: 2635 events with energy above 32 EeV

"Vertical"
2040 with zenith angle θ<60°

"Inclined"
595 with zenith angle θ>60°

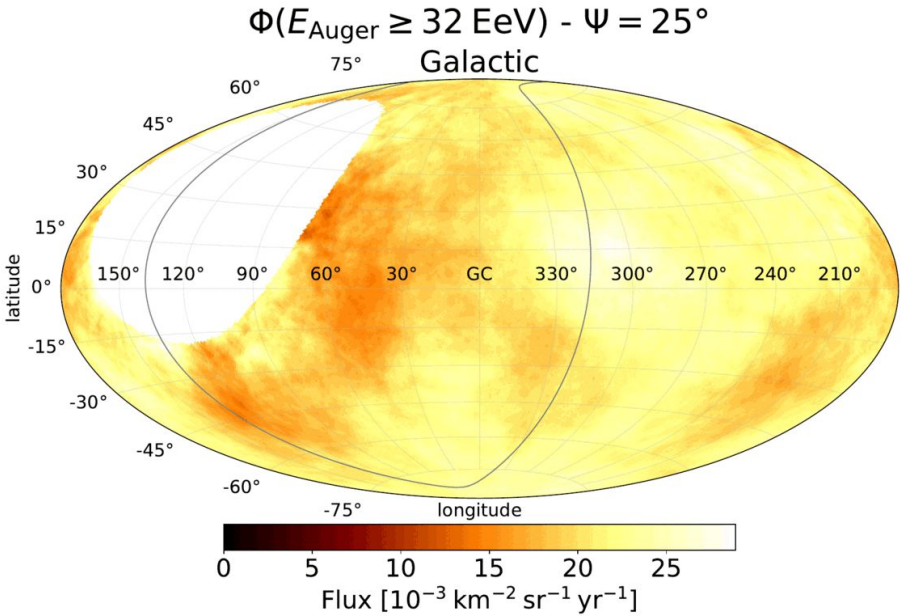

Highest energy range for dipolar searches (where dipole significance drops)

2635 above 32 EeV
647 above 50 EeV
261 above 64 EeV
36 above 100 EeV (0.1 ZeV!)
Highest energy event: 165 EeV

Blind searches for overdensities

Search with little to **no *a priori*** : most prominent overdensity in the whole observable sky

Parameter space is scanned in

- Direction (R.A., Dec)
- Threshold energy Eth = {32, 80} EeV
- Top-Hat angular scale Ψ

Largest significance post-trial **2.2σ**
found at (RA, dec)=(196.3°, -46.6°) or (l, b)=(305.4°, 16.2°)
Nobs = 156 vs Nexp=98 at Eth 41 EeV and Ψ=24°

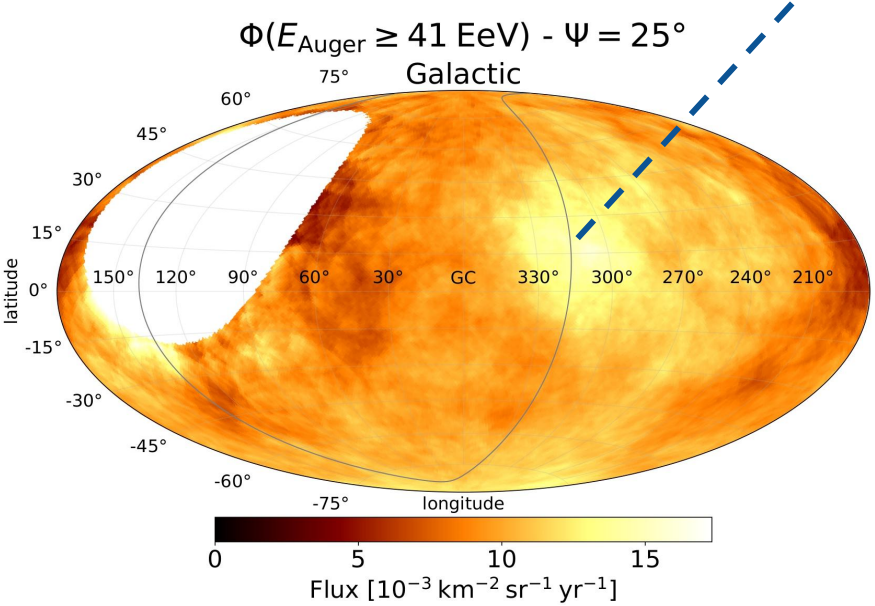

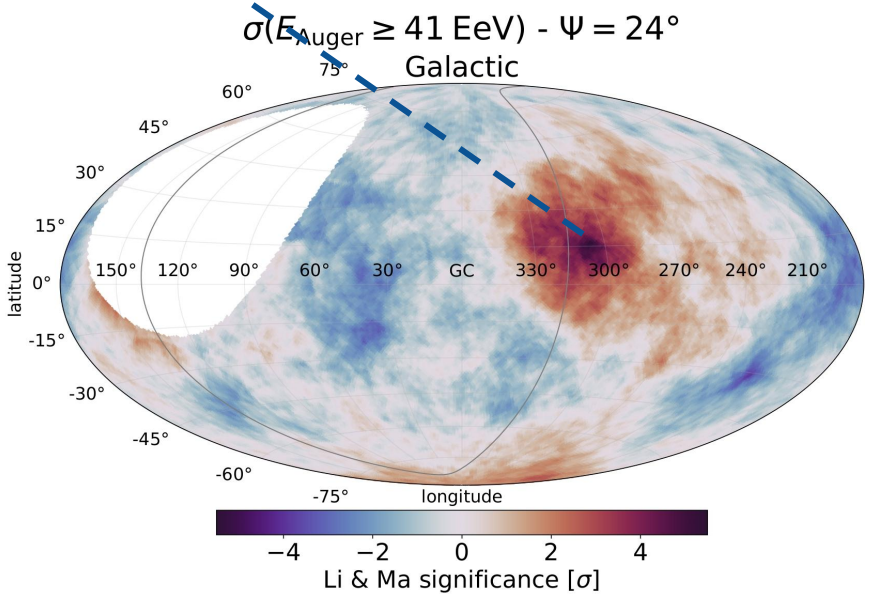

Autocorrelation and correlation with structures

Structures

Events in proximity of local astrophysical structures
Scan in threshold energy, angle Ψ

Autocorrelation

Pairs of events separated by given angular distance
Scan in threshold energy, angle Ψ

Search	E_{th} [EeV]	Angle, Ψ [deg]	N_{obs}	N_{exp}	Local p-value, f_{min}	Post-trial p-value
Autocorrelation	62	3.75	93	66.4	2.5×10^{-3}	0.24
Supergalactic plane	44	20	394	349.1	1.8×10^{-3}	0.13
Galactic plane	58	20	151	129.8	1.4×10^{-2}	0.44
Galactic center	63	18	17	10.1	2.6×10^{-2}	0.57

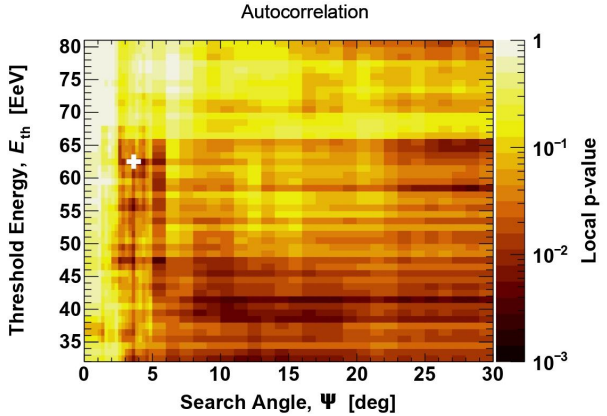

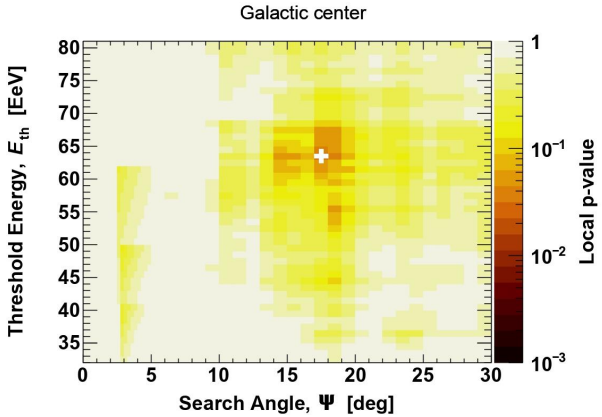

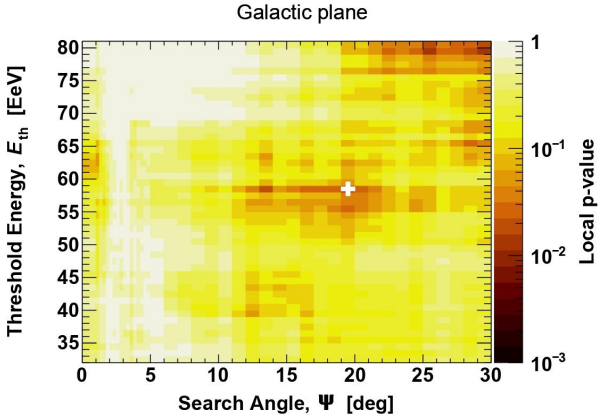

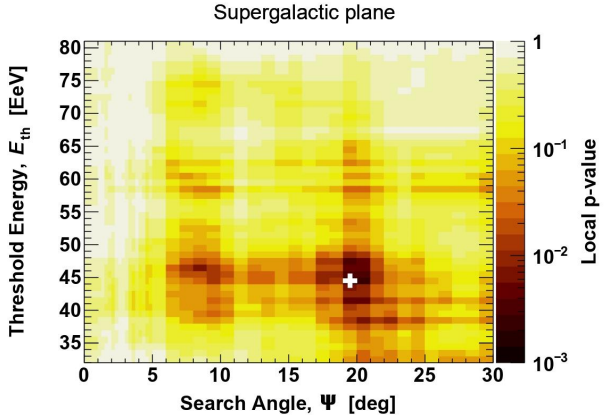

Looking for the sources

CenA, jetted AGN

NGC415, non-jetted AGN

M82, starburst

Electromagnetic emission

EeV cosmic rays

Attenuation weights based on luminosity distance and electromagnetic emission to estimate UHECR flux

Uncut 2MRS catalog color coded in redshift

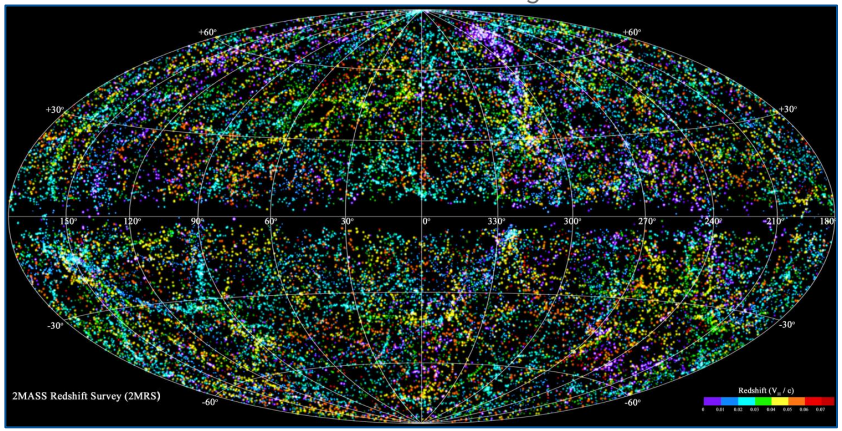

AGN activity

Accretion = X-rays from SwiftBAT (523 galaxies at 14-195 keV)
Jet = γ-rays from 3FHL (26 galaxies at 10 GeV-1 TeV)

Star formation

Generic/**stellar mass = IR** from 2MRS (>40’000 galaxies 2.2 μm)
Burst = radio from Lunardini+19 (44 galaxies, 1.4 GHz)

Result: 4 flux-limited samples - Jetted AGNs, all AGNs, Starburst galaxies, all galaxies

Catalog-based searches

Fit of attenuated flux+isotropy
Variable signal fraction and smoothing scale

All catalogs have most significant signal at Eth=38-41 EeV, scale Ψ=23°-27°, signal fraction α=6-15%

Significance 3.1σ for jetted AGNs,
4.0σ for Starburst galaxies

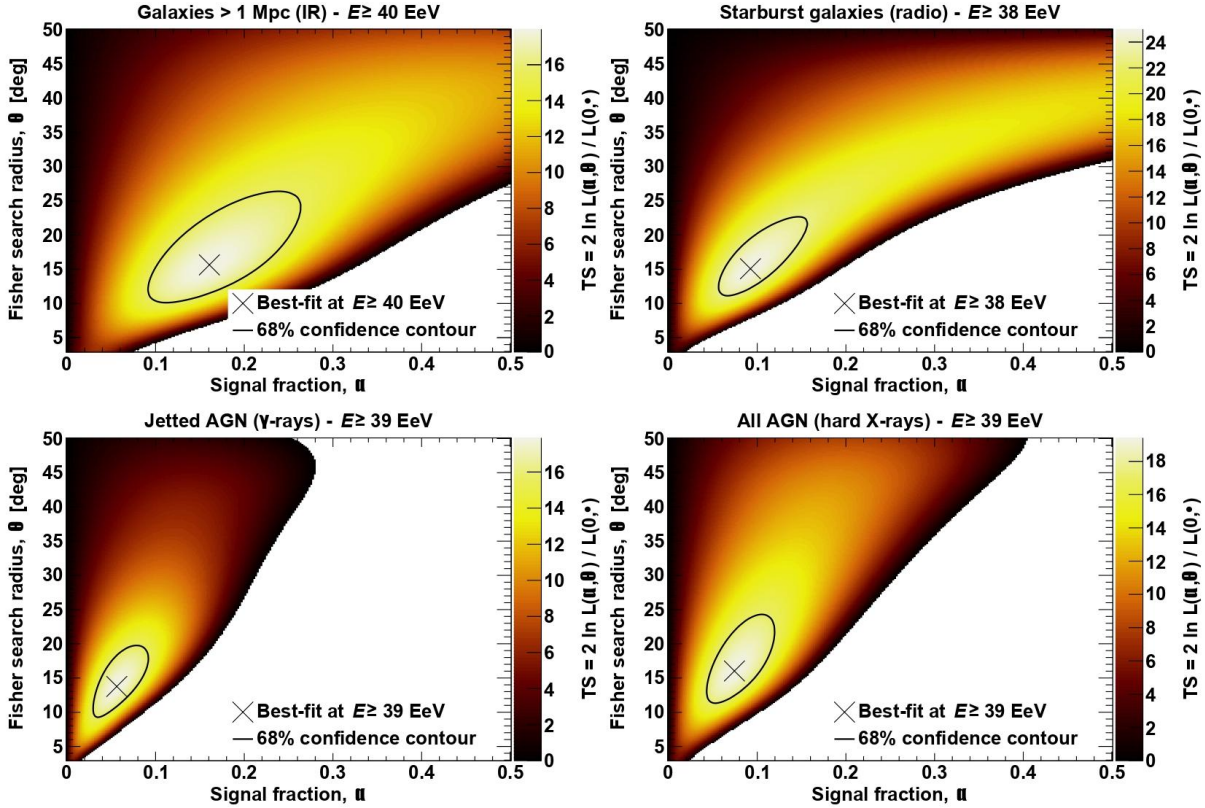

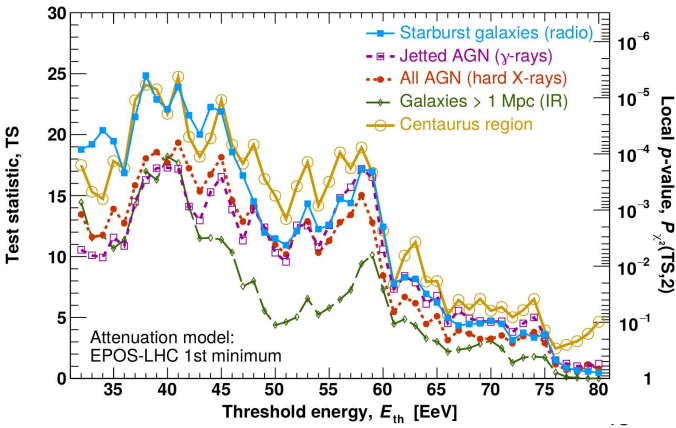

Catalog-based searches

Fit of attenuated flux+isotropy
Variable signal fraction and smoothing scale

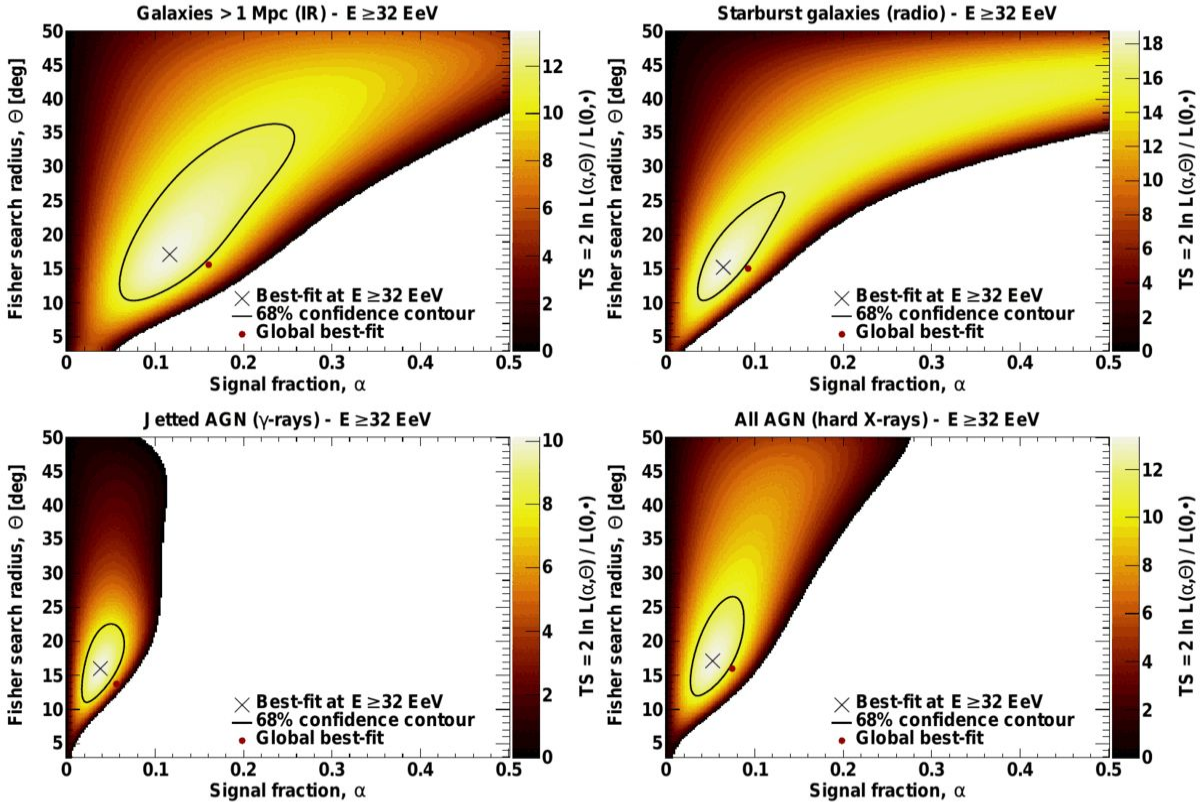

All catalogs have most significant signal at Eth=38-41 EeV, scale Ψ=23°-27°, signal fraction α=6-15%

Significance 3.1σ for jetted AGNs,
4.0σ for Starburst galaxies

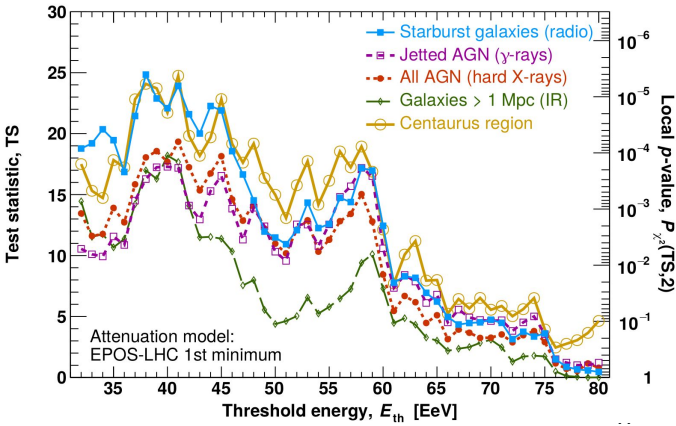

Comparing the sky models

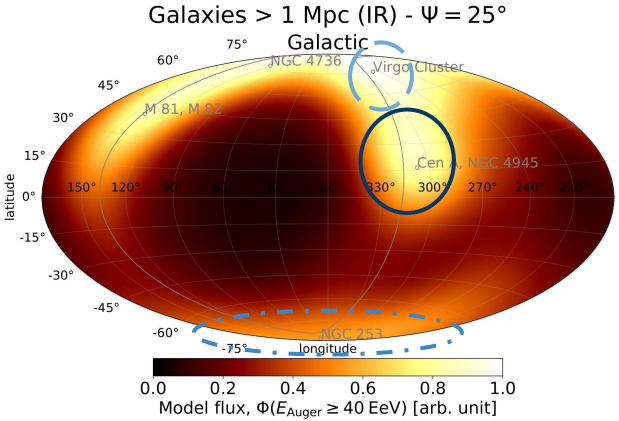

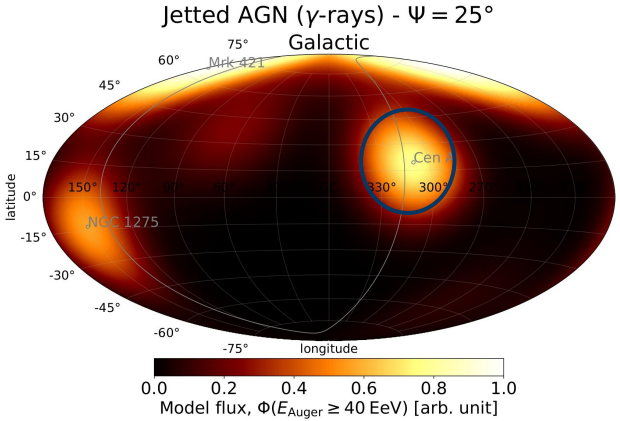

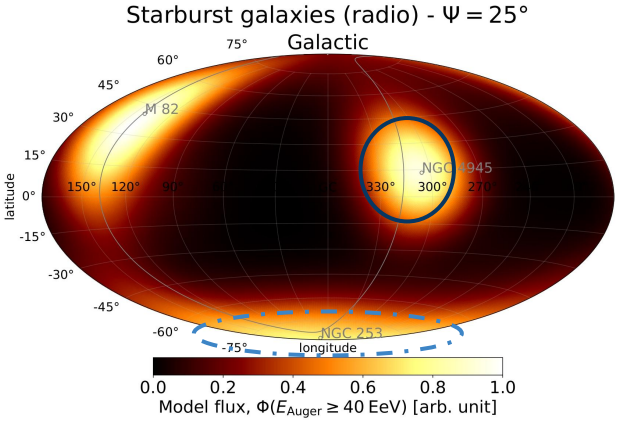

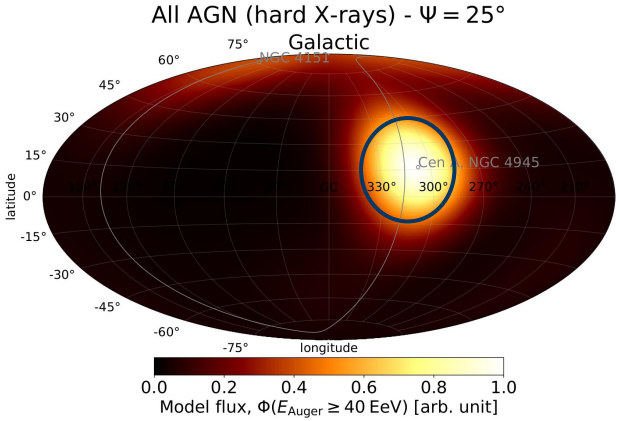

All models capture the hotspot in the **Centaurus region** (M83+NGC4945+CenA)

The starburst model adds the “warm-spot” in the **galactic south pole** (NGC253)

Hotspot missing in the **Virgo Cluster** (l,b) (280°, 75°) in the IR galaxies model

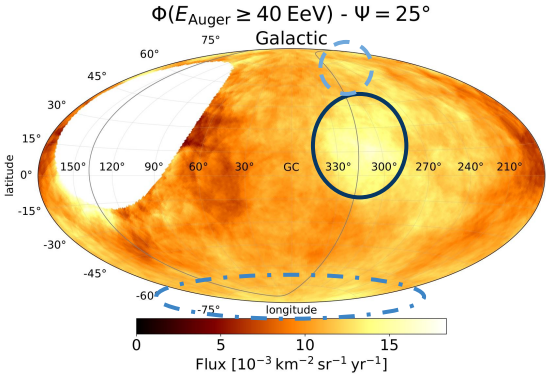

Direct comparison between models shows **mild preference for including** vs excluding **SBGs** (2-3σ)

Excess in the Centaurus region

Motivation

A priori: prominent area in the **Council of Giants**

Flagged area since the first anisotropy results (7% of current exposure)
Most significant overdensity present in the blindsearch
Driving hotspot in all the catalog based models

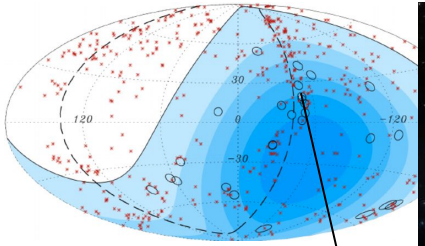

Auger, Science 2007

Direction fixed to CenA, scan in threshold energy and angle Ψ

3.9σ post-trial
for Eth=38 EeV, Ψ=27°

Excess=Nobs-Nexp=215-152=63

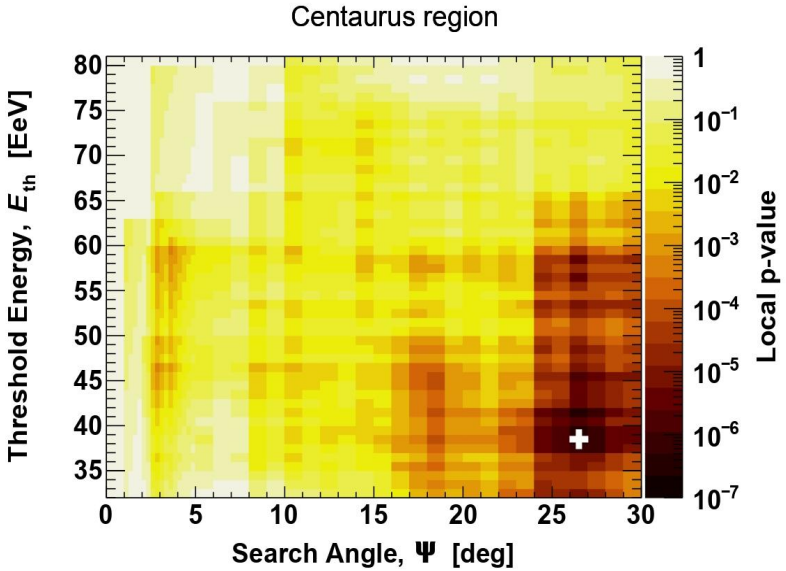

Evolution of signal

Starburst significance was 4.0σ in ApJL2018, 4.5σ at ICRC2019

The drop in significance is mirrored in a plateau of the excess in the Centaurus region

Compatible with linear growth within the expected variance

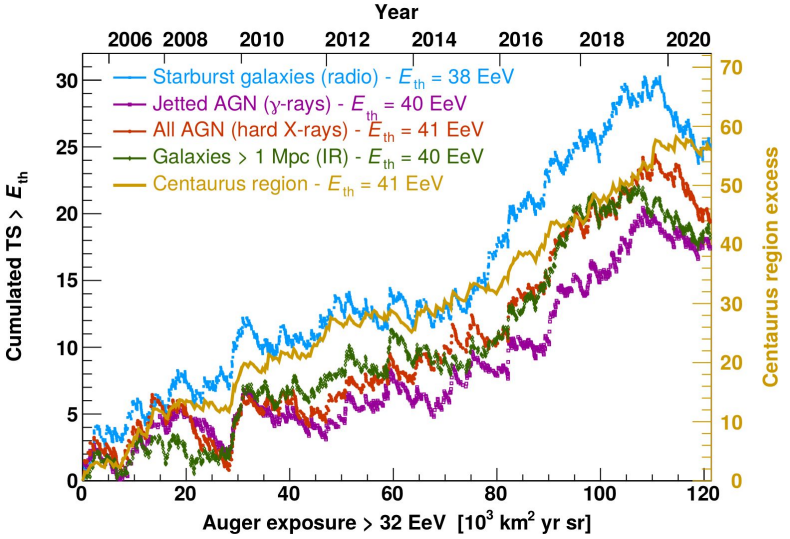

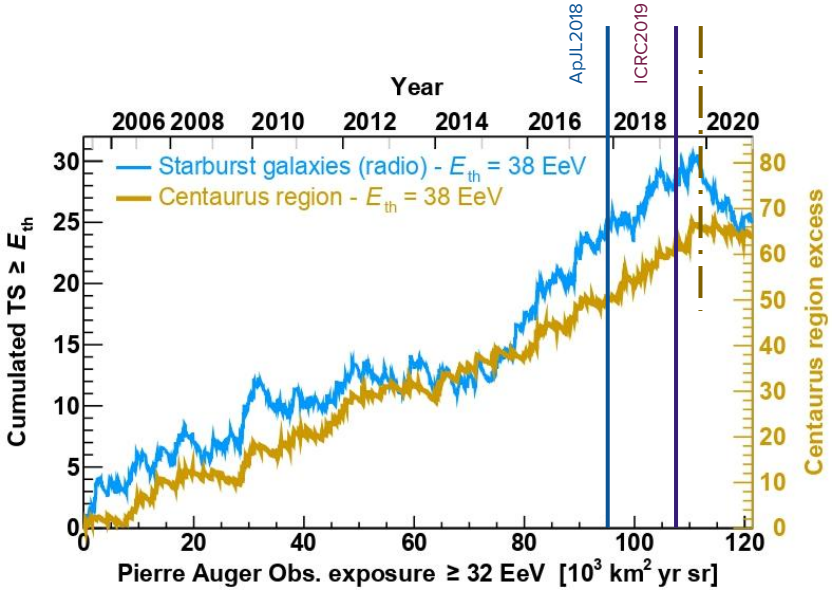

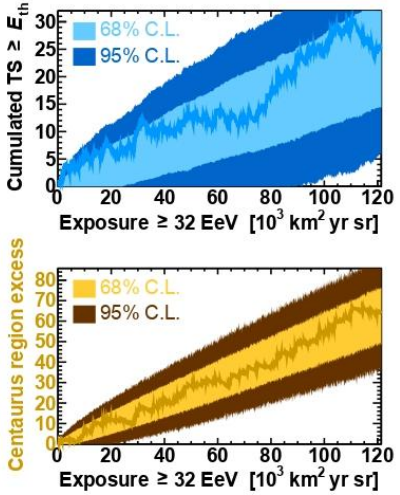

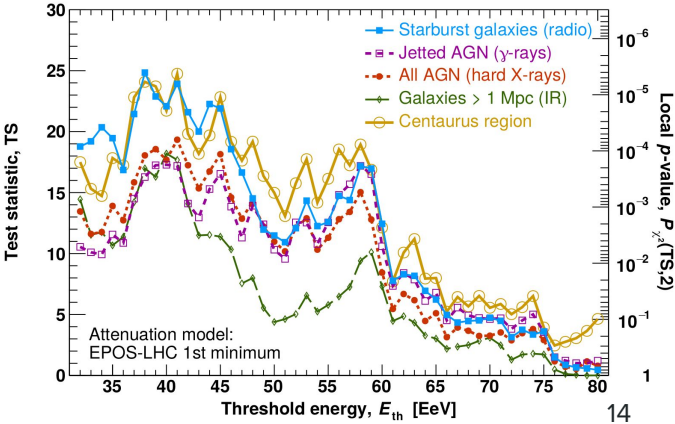

Accessing and using the data and code

https://doi.org/10.5281/zenodo.6504276

The **dataset is available for public use** with the code to reproduce the results

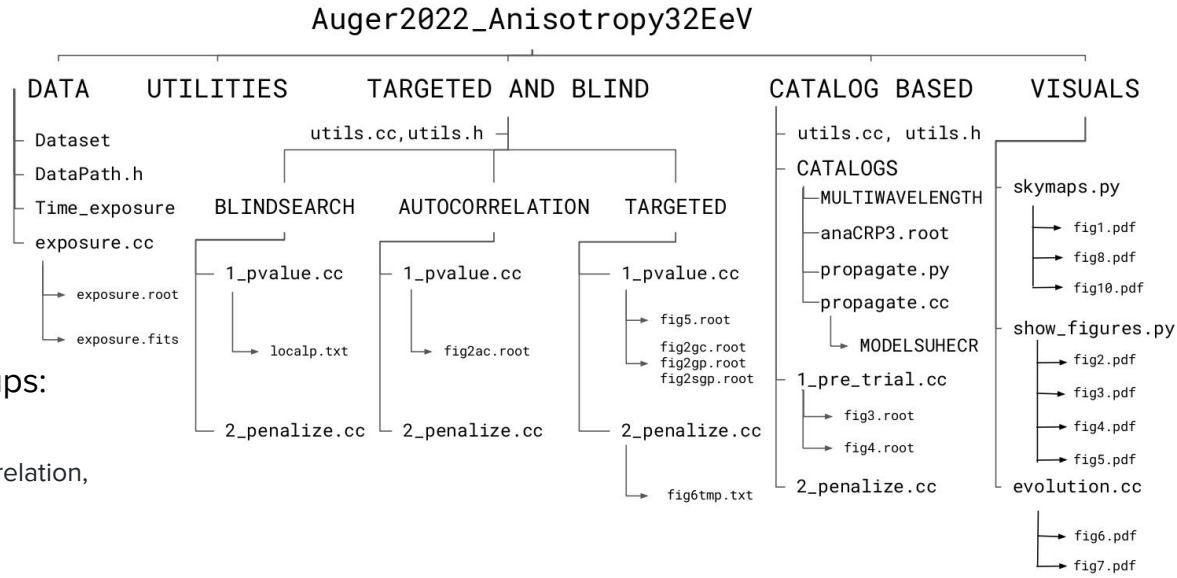

The different analyses are split in two subgroups:

- Targeted and Blind for blindsearch, autocorrelation, astrophysical structures, Centaurus region
- Catalog Based

Requirements: ROOT, HealPix

Plots are produced by the scripts in Visuals

The code adapts to different datasets, provided the source is changed in Data/DataPath.h

Status, and what to do now?

Anisotropies in the toe region with Auger phase 1 data

~4σ from search in Centaurus region, confirmed by catalog-based searches.

Largest signal from starbursts, mild catalog preference compared to others

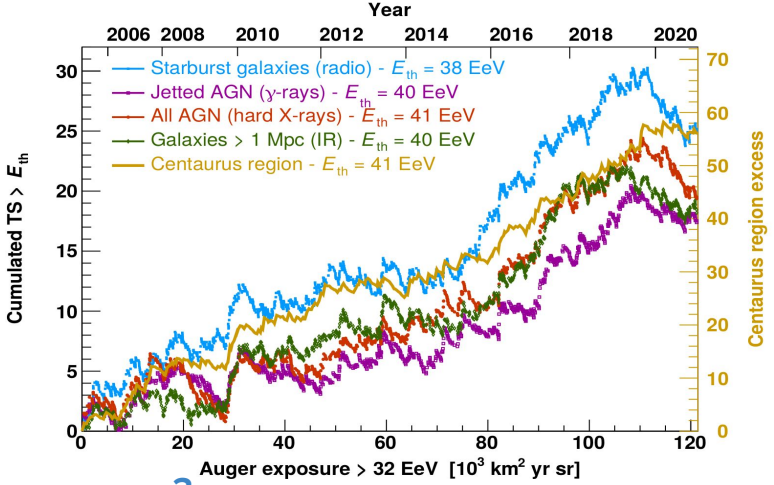

1
Additional information and data

With AugerPrime addition of Xmax information: Select the light component

"Dumb test": removing 25% simulated heaviest component gives 5σ significance in the Centaurus region analysis

TS growth rate ~ 2 units / year (full array)
With TS(5σ) ~ 35
⇒ **Auger-only discovery with current approach in 2025-2030**

2
Full-sky coverage

Auger only sees 85% of the sky

⇒ Combination with Telescope Array (10% of Auger exposure) promising with the upgrades AugerPrime and TAx4

Di Matteo, ICRC2021

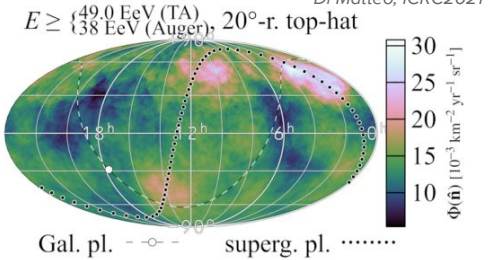

3
Connection with large scales

Interconnection at the instep of the large (ankle) and small/intermediate (toe) scales

Connect sky pattern maps in the local universe with UHECR flux maps

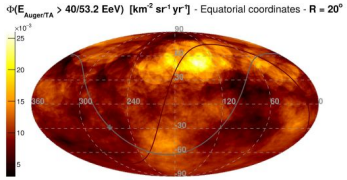

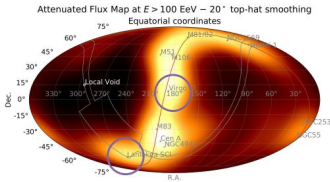

Biteau, ICRC2021

Thank you for your attention

https://doi.org/10.5281/zenodo.6504276

https://arxiv.org/abs/2206.13492

PIERRE AUGER OBSERVATORY

UNIVERSITÀ DEGLI STUDI DI MILANO

Editorial board

Claudio Galelli (Università di Milano)

Lorenzo Caccianiga (INFN Milano)
Jonathan Biteau (Universitè Paris Saclay)
Geraldina Golup (Centro Atomico Bariloche)
Ugo Giaccari (Radboud University Nijmegen)
Paul Sommers (Penn State)
Lorenzo Cazon Boado (Universidade de Santiago de Compostela)

Backup slides

Year	JD	UTC	Zenith angle, θ	Azimuth angle, ϕ	R.A., α	Dec, δ	E	Cumulative exposure
		s	°	°	°	°	EeV	km^2 sr yr
2019	314	1573399408	58.6	−135.6	128.9	−52.0	166	111,900
2007	13	1168768186	14.2	85.6	192.9	−21.2	165	9,800
2020	163	1591895321	18.9	−47.7	107.2	−47.6	155	116,800
2014	293	1413885674	6.8	−155.4	102.9	−37.8	155	70,600
2018	224	1534096475	47.9	141.7	125.0	−0.6	147	101,400
2008	268	1222307719	49.8	140.5	287.8	1.5	140	21,300
2019	117	1556436334	14.8	−32.7	275.0	−42.1	133	107,400
2017	361	1514425553	41.7	−30.5	107.8	−44.7	132	96,100
2014	65	1394114269	58.5	47.3	340.6	12.0	131	65,300
2005	186	1120579594	57.3	155.7	45.8	−1.7	127	3,100
2015	236	1440460829	20.1	−46.1	284.8	−48.0	125	77,700
2008	18	1200700649	50.3	178.9	352.5	−20.8	124	16,100
2016	26	1453874568	22.6	−14.7	175.6	−37.7	122	81,200
2016	21	1453381745	13.7	−179.8	231.4	−34.0	122	81,100
2011	26	1296108817	24.9	90.9	150.0	−10.4	116	39,300
2016	68	1457496302	23.7	108.7	151.5	−12.6	115	82,100
2015	268	1443266386	77.2	−172.0	21.7	−13.8	113	78,400
2016	297	1477276760	49.5	104.5	352.1	13.2	111	86,800
2020	66	1583535647	41.4	−20.6	133.6	−38.3	110	114,600
2018	174	1529810463	42.7	4.3	300.0	−22.6	110	100,200

NOTE—See text for a description of the columns. Events are sorted here by decreasing energy, E, and only the 20 highest-energy events are displayed. The full data set is available in the same format at **DOI 10.5281/zenodo.6504276**.

Likelihood computation

TS evaluation

$$\mathrm{TS} = 2 \sum_i k_i \times \ln \frac{n^{H_1}(\mathbf{u}_i)}{n^{H_0}(\mathbf{u}_i)}. \quad (4)$$

$$n^{H_1}(\mathbf{u}) = (1-\alpha) \times n^{H_0}(\mathbf{u}) + \alpha \times \frac{\sum_j s_j(\mathbf{u};\Theta)}{\sum_i \sum_j s_j(\mathbf{u_i};\Theta)}, \quad (2)$$

Signal fraction

Contribution from each galaxy

$$n^{H_0}(\mathbf{u}) = \frac{\omega(\mathbf{u})}{\sum_i \omega(\mathbf{u}_i)}, \quad (1)$$

Directional exposure of the observatory

$$s_j(\mathbf{u};\Theta) = \omega(\mathbf{u}) \times \phi_j a(d_j) \times \exp\left(\frac{\mathbf{u}\cdot\mathbf{u}_j}{2(1-\cos\Theta)}\right). \quad (3)$$

Count density in the H1 (signal) hypothesis

Count density in the H0 (isotropy) hypothesis

Evolution of signal

Evolution of TS, Signal fraction and search radius as a function of Threshold energy

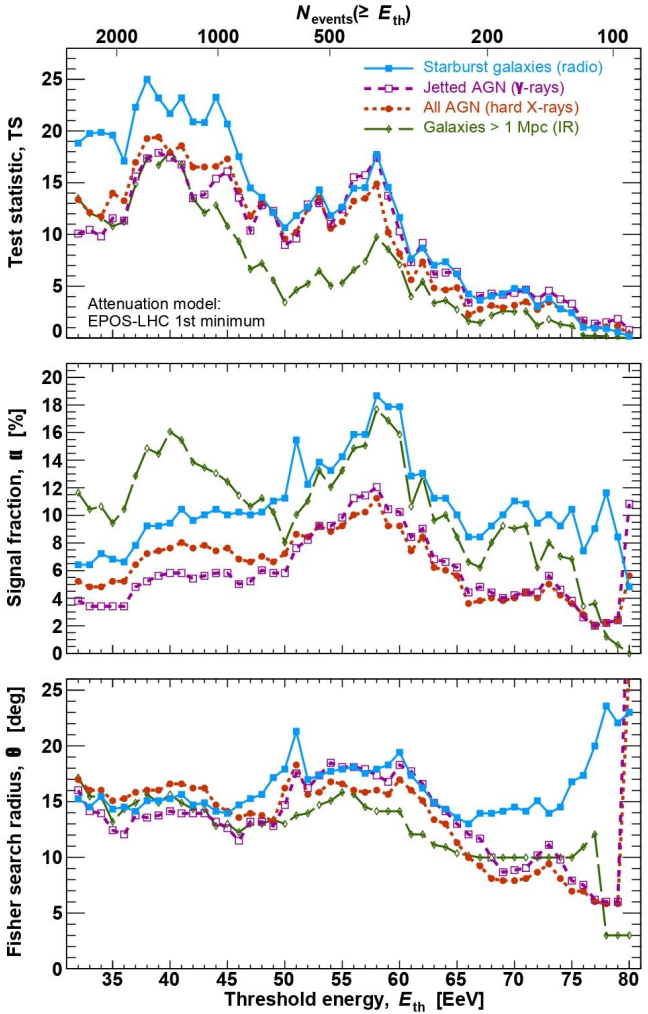

Table 4. Galaxies (2MASS(K<11.75) × HyperLEDA).

PGC	Counterpart	Object Type	R.A.	Dec	$(m-M)$	$\sigma(m-M)$	d_L	$\sigma(d_L)/d_L$	K_t	$\sigma(K_t)$
			°	°	mag	mag	Mpc		mag	mag
29128	NGC3109	G	150.78	-26.16	25.56	0.02	1.29	0.007	9.57	0.4
29653	PGC029653	G	152.75	-4.69	25.59	0.03	1.31	0.013	11.31	0.56
28913	UGC05373	G	150.0	5.33	25.79	0.01	1.44	0.006	10.76	0.23
100169	PGC100169	G	31.52	69.0	26.15	0.2	1.7	0.092	9.69	0.24
67908	IC5152	G	330.67	-51.3	26.46	0.03	1.96	0.012	9.05	0.36
3238	NGC0300	G	13.72	-37.68	26.53	0.02	2.03	0.007	6.58	0.36
1014	NGC0055	G	3.72	-39.2	26.62	0.01	2.11	0.006	6.34	0.18
9140	PGC009140	G	36.18	-73.51	26.63	0.07	2.12	0.032	10.83	0.1
13115	UGC02773	G	53.03	47.79	26.69	0.2	2.18	0.092	9.8	0.1
39573	IC3104	G	184.69	-79.73	26.86	0.02	2.36	0.007	9.24	0.14
60849	IC4662	G	266.79	-64.64	27.03	0.01	2.55	0.006	9.45	0.21
47495	UGC08508	G	202.68	54.91	27.07	0.02	2.6	0.011	11.51	0.1
40904	UGC07577	G	186.92	43.5	27.08	0.02	2.6	0.011	10.45	0.2
54392	ESO274-001	G	228.56	-46.81	27.24	0.06	2.8	0.026	8.3	0.39
51472	UGC09240	G	216.18	44.53	27.25	0.02	2.82	0.008	10.89	0.13
39023	NGC4190	G	183.44	36.63	27.26	0.04	2.83	0.02	11.4	0.77
14241	PGC014241	G	59.96	67.14	27.37	0.03	2.98	0.012	8.24	0.16
4126	NGC0404	G	17.36	35.72	27.37	0.02	2.98	0.007	7.53	0.02
39225	NGC4214	G	183.91	36.33	27.37	0.01	2.98	0.002	8.09	0.21
38881	NGC4163	G	183.04	36.17	27.38	0.02	2.99	0.007	10.92	0.08
15488	NGC1560	G	68.2	71.88	27.38	0.1	2.99	0.046	9.07	0.22
49050	ESO383-087	G	207.32	-36.06	27.52	0.02	3.19	0.007	9.91	0.14
15439	PGC015439	G	68.01	63.62	27.53	0.05	3.2	0.024	10.97	0.17
21396	NGC2403	G	114.21	65.6	27.53	0.01	3.2	0.004	6.24	0.14
47762	NGC5206	G	203.43	-48.15	27.53	0.01	3.21	0.005	8.39	0.25
...	...	...	...	...	...	...	...	...	...	...
127001	PGC127001	G	67.39	-61.25	36.99	0.07	249.7	0.03	11.72	0.18

NOTE—44,113 entries within 250 Mpc. 17,143 entries at $d_L < 100$ Mpc, 39,563 at $d_L < 200$ Mpc.

Table 5. Starburst galaxies (Lunardini+ '19).

Lunardi Name	Counterpart	Host Type	R.A.	Dec	$(m-M)$	$\sigma(m-M)$	d_L	$\sigma(d_L)/d_L$	$\Phi(1.4\,\mathrm{GHz})$	$\sigma(\Phi)$	flag: in Aab+ '18?
			°	°	mag	mag	Mpc		Jy	Jy	(No/Yes/Xcheck)
NGC0055	NGC0055	SBm	3.72	-39.2	26.62	0.01	2.11	0.005	0.37	N/A	N
NGC1569	NGC1569	IB	67.7	64.85	27.53	0.05	3.21	0.023	0.4	N/A	X
NGC2403	NGC2403	SABc	114.21	65.6	27.53	0.01	3.21	0.005	0.39	N/A	X
IC342	IC342	SABc	56.7	68.1	27.68	0.03	3.44	0.014	2.25	N/A	Y
NGC4945	NGC4945	Sbc	196.37	-49.47	27.7	0.02	3.47	0.009	6.6	N/A	Y
NGC3034(M82)	M82	S?	148.97	69.68	27.79	0.01	3.61	0.005	7.29	N/A	Y
NGC0253	NGC253	SABc	11.89	-25.29	27.84	0.02	3.7	0.009	6.0	N/A	Y
N/A	Circinus	Sb	213.29	-65.34	28.12	0.36	4.21	0.166	1.5	N/A	Y
NGC5236(M83)	M83	Sc	204.25	-29.87	28.45	0.02	4.9	0.009	2.44	N/A	Y
Maffei2	Maffei2	Sbc	40.48	59.6	28.79	0.12	5.73	0.055	1.01	N/A	X
NGC6946	NGC6946	SABc	308.72	60.15	29.14	0.05	6.73	0.023	1.4	N/A	Y
NGC4631	NGC4631	SBcd	190.53	32.54	29.33	0.02	7.35	0.009	1.12	N/A	Y
NGC5194(M51)	M51	SABb	202.48	47.2	29.67	0.02	8.59	0.009	1.31	N/A	Y
NGC5055(M63)	NGC5055	Sbc	198.96	42.03	29.78	0.01	9.04	0.005	0.35	N/A	Y
NGC2903	NGC2903	Sbc	143.04	21.5	29.85	0.11	9.33	0.051	0.44	N/A	Y
NGC891	NGC891	Sb	35.64	42.35	29.94	1.72	9.73	0.792	0.7	N/A	Y
NGC1068	NGC1068	Sb	40.66	0.0	30.12	0.34	10.6	0.157	4.85	N/A	Y
NGC3628	NGC3628	SBb	170.07	13.59	30.21	0.34	11.0	0.157	0.47	N/A	Y
NGC4818	NGC4818	SABa	194.2	-8.53	30.27	0.33	11.3	0.152	0.45	N/A	N
NGC3627	NGC3627	Sb	170.06	12.99	30.3	0.04	11.5	0.018	0.46	N/A	Y
NGC1808	NGC1808	Sa	76.93	-37.51	30.45	0.36	12.3	0.166	0.5	N/A	X
NGC4303	M61	Sbc	185.48	4.47	30.45	0.1	12.3	0.046	0.44	N/A	X
NGC3521	NGC3521	SABb	166.45	-0.04	30.47	0.29	12.4	0.134	0.35	N/A	N
NGC0660	NGC660	Sa	25.76	13.65	30.5	1.31	12.6	0.603	0.37	N/A	Y
NGC4254	NGC4254	Sc	184.71	14.42	30.77	1.13	14.3	0.52	0.37	N/A	N
...	...	...	...	...	...	...	...	...	...	...	...
NGC6240	NGC6240	S0-a	253.26	2.4	35.18	0.15	108.6	0.069	0.65	N/A	Y

NOTE—44 entries within 250 Mpc. 43 entries at $d_L < 100$ Mpc, 44 at $d_L < 200$ Mpc.

Table 6. Jetted and non-jetted AGNs (*Swift*-BAT 105 months).

BAT105 Name	Counterpart	AGN Type	R.A.	Dec	$(m-M)$	$\sigma(m-M)$	d_L	$\sigma(d_L)/d_L$	$\Phi(14-195\,\mathrm{keV})$	$\sigma(\Phi)$	flag: ref. $(m-M)$
			°	°	mag	mag	Mpc		$10^{-12}\,\mathrm{erg\,cm^{-2}\,s^{-1}}$	$10^{-12}\,\mathrm{erg\,cm^{-2}\,s^{-1}}$	(HyperLEDA/NED)
J1305.4-4928	NGC4945	Sy2	196.37	-49.47	27.7	0.02	3.47	0.009	282.1	N/A	H
J0955.5+6907	M81	Sy1.9	148.94	69.06	27.78	0.01	3.6	0.005	20.3	N/A	H
J1325.4-4301	CenA	BeamedAGN	201.37	-43.02	27.83	0.03	3.68	0.014	1346.3	N/A	H
J1412.9-6522	Circinus	Sy2	213.29	-65.34	28.12	0.36	4.21	0.166	273.2	N/A	H
J1210.5+3924	NGC4151	Sy1.5	182.64	39.41	28.39	1.65	4.76	0.76	618.9	N/A	H
J1202.5+3332	NGC4395	Sy2	186.45	33.53	28.39	0.01	4.76	0.005	27.5	N/A	H
J0420.0-5457	NGC1566	Sy1.5	64.96	-54.94	29.13	1.16	6.7	0.534	19.5	N/A	H
J1219.4+4720	M106	Sy1.9	184.75	47.29	29.41	0.01	7.62	0.005	23.0	N/A	H
J1329.9+4719	M51	Sy2	202.48	47.2	29.67	0.02	8.59	0.009	13.3	N/A	H
J0242.6+0000	NGC1068	Sy1.9	40.66	0.0	30.12	0.34	10.6	0.157	37.9	N/A	H
J1717.1-6249	NGC6300	Sy2	259.25	-62.83	30.15	0.09	10.7	0.041	96.4	N/A	H
J1203.0+4433	NGC4051	Sy1.5	180.78	44.52	30.28	0.35	11.4	0.161	42.5	N/A	H
J1652.0-5915B	NGC6221	Sy2	253.18	-59.23	30.34	0.62	11.7	0.286	22.4	N/A	H
J1209.4+4340	NGC4138	Sy2	182.35	43.7	30.7	0.25	13.8	0.115	24.4	N/A	H
J1157.8+5529	NGC3998	Sy1.9	179.46	55.44	30.73	0.19	14.0	0.087	13.2	N/A	H
J2235.9-2602	NGC7314	Sy1.9	338.95	-26.05	31.03	0.25	16.1	0.115	57.4	N/A	H
J1432.8-4412	NGC5643	Sy2	218.19	-44.15	31.03	1.0	16.1	0.461	16.8	N/A	H
J1001.7+5543	NGC3079	Sy2	150.46	55.67	31.16	0.32	17.1	0.147	36.7	N/A	H
J1341.9+3537	NGC5273	Sy1.5	205.47	35.66	31.16	0.12	17.1	0.055	16.0	N/A	H
J1207.8+4311	NGC4117	Sy2	181.95	43.12	31.18	0.94	17.2	0.433	12.9	N/A	H
J0333.6-3607	NGC1365	Sy2	53.39	-36.14	31.19	0.02	17.3	0.009	63.5	N/A	H
J0241.3-0816	NGC1052	BeamedAGN	40.29	-8.24	31.22	0.11	17.5	0.051	31.4	N/A	H
J1132.7+5301	NGC3718	Sy1.9	173.22	53.02	31.25	0.89	17.8	0.41	12.2	N/A	H
J1206.2+5243	NGC4102	Sy2	181.59	52.71	31.29	0.25	18.1	0.115	32.1	N/A	H
J2318.4-4223	NGC7582	Sy2	349.6	-42.37	31.41	0.1	19.1	0.046	82.3	N/A	H
...	...	...	...	...	...	...	...	...	...	...	...
J0534.8-6026	2MASXJ05343093-6016153	Sy1	83.7	-60.27	36.98	0.06	248.9	0.028	10.7	N/A	H

NOTE—523 entries within 250 Mpc. 201 entries at $d_L < 100$ Mpc, 458 at $d_L < 200$ Mpc.

Table 7. Jetted AGNs (*Fermi*-LAT 3FHL).

3FHL Name	Counterpart	Jetted AGN Type	R.A.	Dec	$(m-M)$	$\sigma(m-M)$	d_L	$\sigma(d_L)/d_L$	$\Phi(0.01-1\ \mathrm{TeV})$	$\sigma(\Phi)$	flag: in Aab+ '18?
			°	°	mag	mag	Mpc		$10^{-10}\ \mathrm{cm^{-2}\ s^{-1}}$	$10^{-10}\ \mathrm{cm^{-2}\ s^{-1}}$	(No/Yes)
J1325.5-4300	CenA	RDG	201.37	-43.02	27.83	0.03	3.68	0.014	1.54	0.25	Y
J1230.8+1223	M87	RDG	187.71	12.39	31.12	0.06	16.7	0.028	0.98	0.2	Y
J0322.6-3712e	FornaxA	RDG	50.67	-37.21	31.55	0.03	20.4	0.014	0.48	0.16	N
J1346.2-6026	CenB	RDG	206.7	-60.41	33.71	0.29	55.2	0.134	0.64	0.18	N
J0319.8+4130	NGC1275	RDG	49.95	41.51	34.46	0.08	78.0	0.037	14.17	0.67	Y
J0316.6+4120	IC310	RDG	49.18	41.32	34.6	0.19	83.2	0.087	0.43	0.13	Y
J0153.5+7115	TXS0149+710	BCU	28.36	71.25	35.07	0.15	103.3	0.069	0.44	0.12	Y
J0308.4+0408	NGC1218	RDG	47.11	4.11	35.48	0.13	124.7	0.06	0.54	0.16	N
J1104.4+3812	Mkn421	BLL	166.1	38.21	35.63	0.12	133.7	0.055	59.35	1.38	Y
J1653.8+3945	Mkn501	BLL	253.47	39.76	35.91	0.1	152.1	0.046	19.17	0.76	Y
J0131.1+5546	TXS0128+554	BCU	22.81	55.75	36.06	0.1	162.9	0.046	0.33	0.12	N
J1543.6+0452	CGCG050-083	BCU	235.89	4.87	36.26	0.09	178.6	0.041	0.69	0.17	N
J0223.0-1119	1RXSJ022314.6-111741	BLL	35.81	-11.29	36.31	0.09	182.8	0.041	0.4	0.13	N
J2347.0+5142	1ES2344+514	BLL	356.76	51.69	36.47	0.08	196.8	0.037	3.32	0.31	Y
J0816.4-1311	PMNJ0816-1311	BLL	124.11	-13.2	36.51	0.08	200.4	0.037	2.71	0.33	N
J1136.5+7009	Mkn180	BLL	174.11	70.16	36.54	0.08	203.2	0.037	1.74	0.21	Y
J1959.9+6508	1ES1959+650	BLL	299.97	65.16	36.63	0.08	211.8	0.037	8.43	0.46	Y
J1647.6+4950	SBS1646+499	BLL	251.9	49.83	36.64	0.08	212.8	0.037	0.48	0.12	N
J1517.6-2422	APLibrae	BLL	229.42	-24.37	36.68	0.07	216.8	0.032	3.76	0.37	Y
J0214.5+5145	TXS0210+515	BLL	33.55	51.77	36.7	0.11	218.8	0.051	0.42	0.12	Y
J1806.8+6950	3C371	BLL	271.71	69.82	36.77	0.07	225.9	0.032	1.3	0.18	N
J1353.0-4413	PKS1349-439	BLL	208.24	-44.21	36.79	0.07	228.0	0.032	0.33	0.12	N
J0200.1-4109	1RXSJ020021.0-410936	BLL	30.09	-41.16	36.85	0.07	234.4	0.032	0.51	0.14	N
J0627.1-3528	PKS0625-35	BLL	96.78	-35.49	36.89	0.07	238.8	0.032	1.81	0.26	Y
J2039.4+5219	1ES2037+521	BLL	309.85	52.33	36.89	0.07	238.8	0.032	0.58	0.15	N
J0523.0-3627	PKS0521-36	BLL	80.76	-36.46	36.91	0.07	241.0	0.032	1.17	0.21	N

NOTE—26 entries within 250 Mpc. 6 entries at $d_L < 100$ Mpc, 14 at $d_L < 200$ Mpc.

Jetted AGN model (EPO1st)

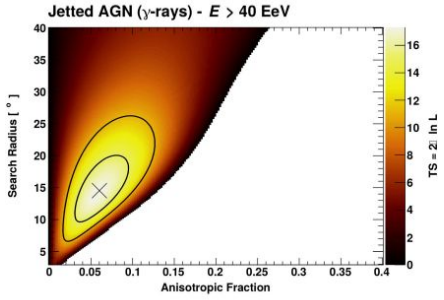

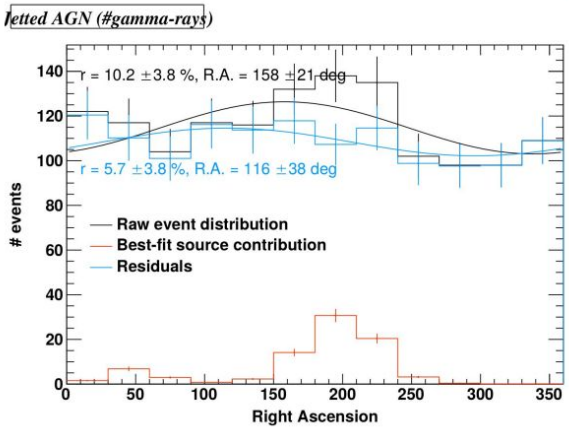

Note: 2MRS dipole at R.A. ~ 155°

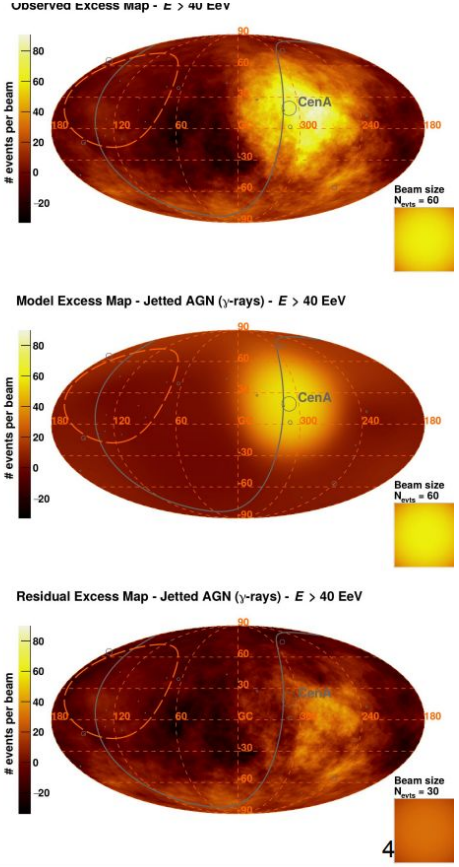

Courtesy of J. Biteau

All AGN model (EPO1st)

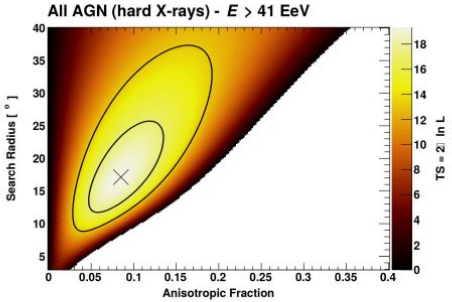

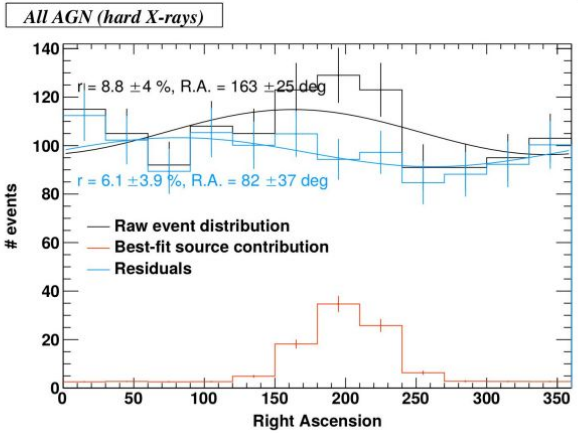

Note: 2MRS dipole at R.A. ~ 155°

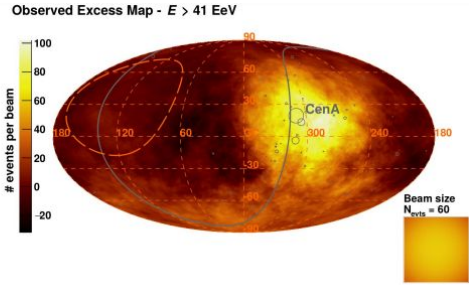

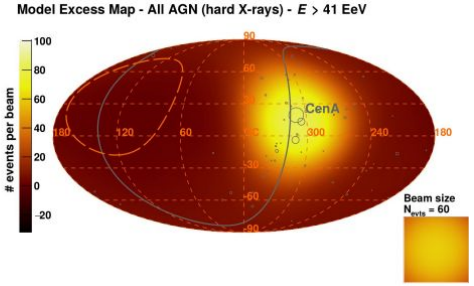

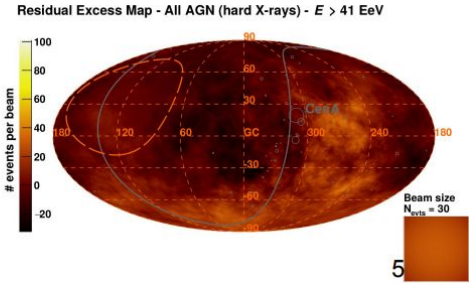

Courtesy of J. Biteau

Starburst model (EPO1st)

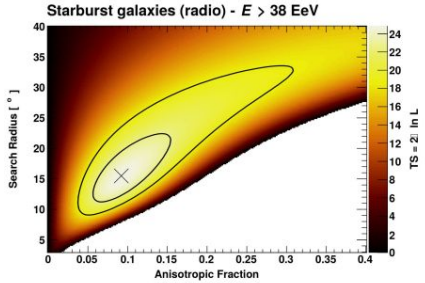

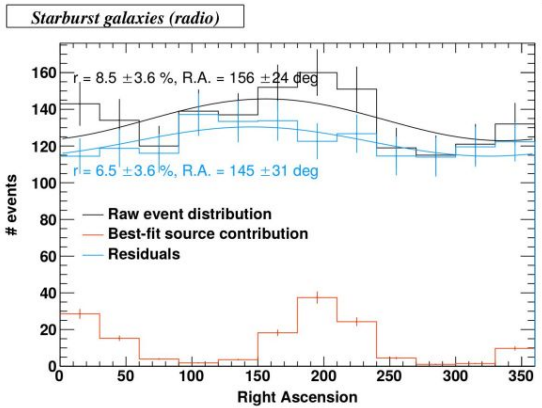

Note: 2MRS dipole at R.A. ~ 155°

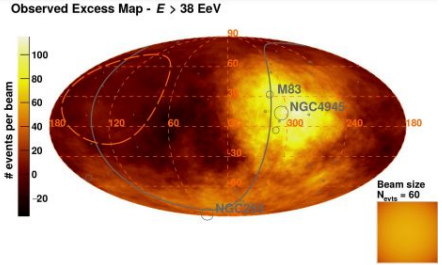

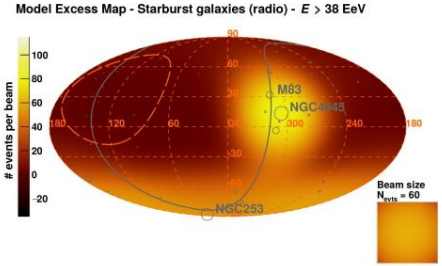

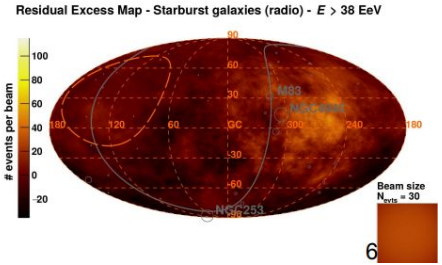

Courtesy of J. Biteau

All Galaxies model (EPO1st)

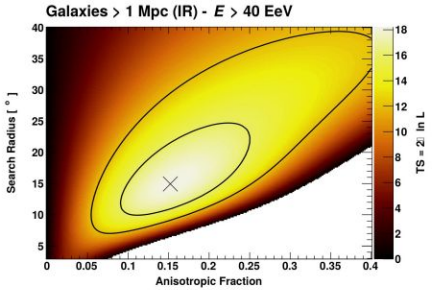

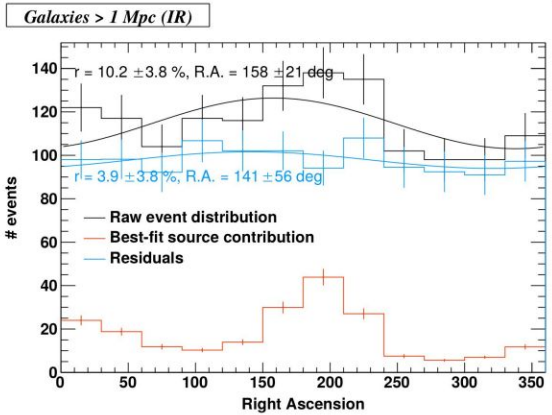

Note: 2MRS dipole at R.A. ~ 155°

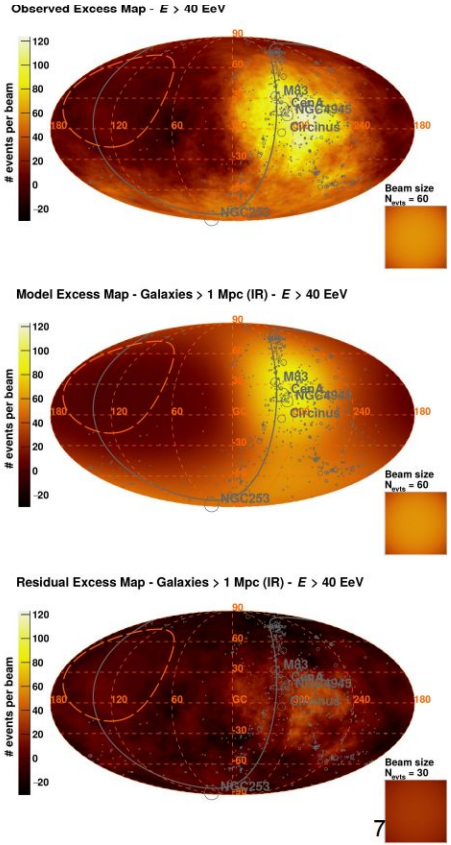

Courtesy of J. Biteau

Summary

amplitude	**Intermediate-scale signal, α**	**Large-scale R.A. residual modulation, r**
SBG	9%	7%
All Galaxies	15%	4%
Jetted AGN	6%	6%
All AGNs	8%	6%
typical uncertainty	± 5%	± 4%

pros/cons	**Intermediate-scale signal, α**	**Large-scale R.A. residual modulation, r**
SBG	Best match (TS~25)	Inferior match (r=0 within 1.5-2σ) Compatible with 2MRS
All Galaxies	Inferior match (TS~18) due to Virgo excess	Best match (r=0 within 1σ)
Jetted AGN	Inferior match (TS~17) due tepid spot deficit	Inferior match (r=0 within 1.5) Incompatible with 2MRS
All AGNs	Inferior match (TS~19) due tepid spot deficit	Inferior match (r=0 within 1.5) Compatible with 2MRS